ORGANIC CHEMISTRY FRONTIERS

RESEARCH ARTICLE

View Article Online
View Journal | View Issue

Cite this: *Org. Chem. Front.*, 2021, **8**, 1424

Reversible fluorescence modulation through the photoisomerization of an azobenzene-bridged perylene bisimide cyclophane†

Guanghui Ouyang,[a,b] David Bialas[a] and Frank Würthner *[a]

Received 25th December 2020,
Accepted 2nd February 2021

DOI: 10.1039/d0qo01635g

rsc.li/frontiers-organic

A new type of perylene bisimide (PBI) cyclophane in which two PBI chromophores were linked *via* an azobenzene (Azo) bridge was designed and synthesized. It was found that the integration of electron-donating azobenzene and electron-deficient PBI in a well-defined cyclophane enables the regulation of the fluorescence lifetime and quantum yield of the PBI units. With the aid of a high efficiency *trans* → *cis* transformation of the azobenzene moiety, the PBI–PBI chromophore distance can be effectively controlled as revealed by exciton coupling and density functional theory (DFT) computation, leading to additional non-radiative decay pathways and a pronounced fluorescence quenching due to cooperative adjustments of PBI–PBI and PBI–Azo interactions. Reversible fluorescence intensity switching for at least five cycles was successfully achieved with alternate UV and visible light irradiation. These well-controlled fluorescence modulation and photoswitching behaviours not only provide insights into interchromophoric interactions but also contribute to the development of stimuli-responsive luminescent macrocycles.

Introduction

Macrocycles and cyclophanes,[1–3] developed by Cram, Lehn and Pederson for molecular recognition, constitute the first examples of synthetic supramolecular elements.[4] More recently, to meet the developing requirements of smart supramolecular materials,[5–9] dynamic macrocycles and cyclophanes responding to external stimuli have gained increasing attention due to their key roles in designing smart fluorescent materials,[10–13] molecular machines,[14] and controlled supramolecular transport systems.[15,16] However, among the reported stimuli-responsive macrocycles, dynamic cyclophanes are less studied,[17,18] partly due to their relatively rigid conformations and synthetic challenges from the build-up of strain.

PBI-based cyclophanes are of particular interest due to the high photoluminescence quantum yield and robust photo and chemical stability of PBIs.[19,20] However, because of the poor solubility and strong aggregation tendency of unsubstituted PBIs, the synthesis of PBI cyclophanes is quite challenging and only a few examples have been reported so far (Fig. 1a).[21–25] Furthermore, due to the strong attraction of PBIs, there are no cavities provided by these cyclophanes for the complexation of guest molecules. Only in 2015, our group successfully reported a new type of PBI cyclophane bearing an open cavity by utilizing tetra-*tert*-butylphenoxy substituted perylene bisanhydride as an easily soluble precursor and toluene as the solvent and template for the cyclization reaction.[26] Based on this high efficiency cyclization method, a PBI cyclophane library was established by our group using various CH_2–arylene–CH_2 linkers.[27–31] The structure–property investigation of this PBI cyclophane library clearly clarified that the length of the linker could effectively control the interchromophoric distances and therefore significantly affect both PBI–PBI interactions and recognition properties for polycyclic aromatic hydrocarbon guest molecules.[26,28,32] Inspired by these discoveries, we envisioned a dynamic PBI cyclophane by using a photoresponsive moiety as a linker, which is expected to reversibly regulate the PBI–PBI interchromophoric interactions and further modulate the fluorescence properties of the PBI units. Accordingly, the family of PBI cyclophanes could be enriched with a new supramolecular element that is the first one bearing a light-switchable architecture (Fig. 1b).

Thus, we herein report a dynamic supramolecular macrocycle by the cyclization of two azobenzene moieties and two PBI luminophores into cyclophane **APC** (Azo-PBI cyclophane), whose fluorescence intensity can be reversibly regulated under UV and visible light irradiation. At the thermal equilibrium state, both azobenzene units are mainly in the *trans*-configuration. The relatively long molecular length of *trans*-Azo led to

[a]*Institut für Organische Chemie and Center for Nanosystems Chemistry, Universität Würzburg, Am Hubland, 97074 Würzburg, Germany.*
E-mail: wuerthner@uni-wuerzburg.de
[b]*CAS Key Laboratory of Colloid, Interface and Chemical Thermodynamics, Institute of Chemistry, Chinese Academy of Sciences, ZhongGuanCun, North First Street 2, 100190 Beijing, China*

†Electronic supplementary information (ESI) available. See DOI: 10.1039/d0qo01635g

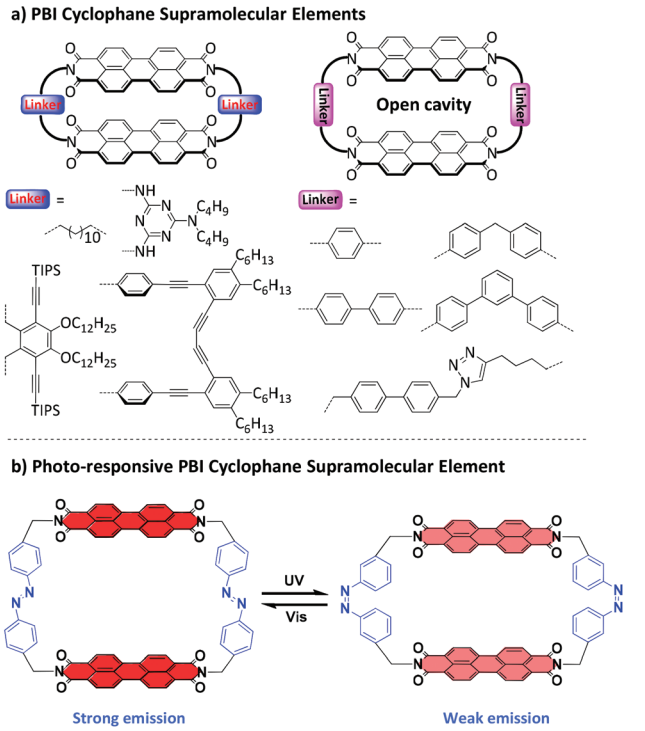

Fig. 1 Schematic illustration of PBI cyclophane supramolecular elements. (a) Representative PBI cyclophane supramolecular elements with rigid linkers. (b) PBI cyclophane supramolecular element with photoresponsive linkers, which showed reversible structural and fluorescence switching under alternate UV and visible light irradiation. Notes: The bay-position substituents of the PBIs are omitted for clarity. For details of the PBI cyclophane structures illustrated in (a), the original literature reports[21–25] should be consulted.

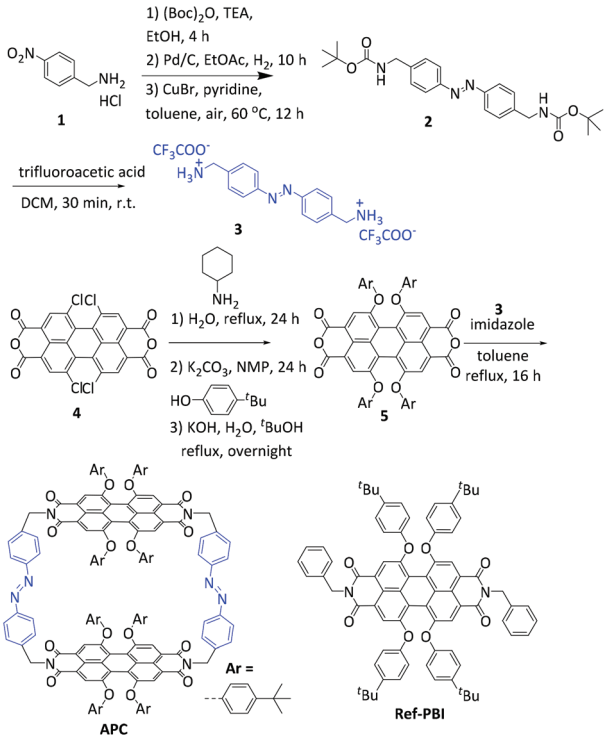

Scheme 1 The synthetic route towards PBI cyclophane **APC**. In addition, the chemical structure of **Ref-PBI**[27] is shown, which is used as a reference compound.

the formation of a large cavity for the cyclophane, resulting in weak exciton coupling between the PBI units.[33,34] Under UV irradiation (λ_{ex} = 350 nm) for several seconds, the azobenzene groups undergo a *trans* → *cis* transformation, resulting in the formation of a photostationary state of **APC** (PSS-**APC**). Such a light-initialized isomerization process effectively changed the molecular geometry and electronic properties of **APC**. As a result, the FLQY and fluorescence intensity of PSS-**APC** weakened compared with those of its *trans–trans* counterpart due to cooperative adjustments of PBI–PBI and PBI–Azo interactions. Back-switching from PSS-**APC** to the initial *trans–trans* **APC** (abbreviated as *trans*-**APC**) could be realized by visible light irradiation. Up to five cycles of fluorescence switching using alternate UV and visible light irradiation proved to be a macrocycle fluorescence switch with fatigue resistance, which might enable potential applications in smart photoresponsive fluorescent probes and controlled supramolecular transport systems.

Results and discussion

APC was synthesized according to the route shown in Scheme 1 and S1 (ESI†). The two precursor components, azobenzene diamine **3**[35] and perylene bisanhydride **5**,[36–38] were synthesized following literature-known procedures. Equal equivalents of **3** and **5** were then refluxed in anhydrous toluene under a nitrogen atmosphere for 16 h in the presence of an excess amount of imidazole. After purification by flash column chromatography and recycling gel permeation chromatography, **APC** was obtained as a red-brown solid in a yield of 25%. **APC** was characterized by its melting point, and ^{1}H-NMR, ^{13}C-NMR spectroscopy and high-resolution mass spectrometry (Fig. S1–4, ESI†).

First, UV/Vis spectra of reference compounds **2** and **Ref-PBI** (for the chemical structure, see Scheme 1) were recorded to investigate the optical properties of the pristine linker and PBI moiety. The absorption maximum of **Ref-PBI** in dichloromethane is located at 588 nm with a vibronic progression at 547 nm (Fig. 2a, blue line, and Table 1). Furthermore, an additional absorption band is present at 454 nm, which can be assigned to the $S_0 \rightarrow S_2$ transition.[27] In contrast, reference azobenzene **2** shows significant absorption at shorter wavelengths with a maximum at 343 nm (Fig. 2a, black line), whereas **Ref-PBI** shows only weak absorption. Hence, a selective excitation of the azobenzene moiety can be realized in the presence of a PBI chromophore. The validity of this strategy is well proven by control experiments. As shown in Fig. S7 (ESI†), 350 nm UV irradiation of a mixture of **2**/**Ref-PBI** (1 : 1 in molar ratio) led to a significant decrease of *trans*-azobenzene absorption at 343 nm, which is a signature for the *trans* → *cis* transformation

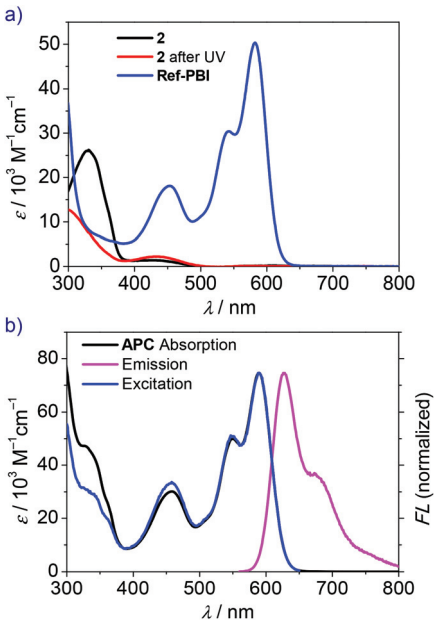

Fig. 2 Spectroscopic study of reference compounds and **APC**. (a) UV-vis absorption spectrum of **Ref-PBI** (blue line) and reference azobenzene **2** before (black line) and after UV irradiation for 1 min (red line) at 298 K, [**Ref-PBI**] = [**2**] = 5.0×10^{-6} M in DCM. (b) UV-vis absorption (black line), fluorescence (λ_{ex} = 550 nm, magenta line) and excitation spectra (λ_{ex} = 670 nm, scan from 300 to 650 nm, blue line) of **APC** at 298 K, [**APC**] = 5.0×10^{-6} M in $CHCl_3$.

Table 1 Absorption and fluorescence properties of **APC** in dichloromethane

	Trans-**APC**	PSS-**APC**[a]	**Ref-PBI**[26]
$\lambda_{abs}(A_{0-0})$/nm	583	586	588
$\lambda_{abs}(A_{0-1})$/nm	545	548	547
A_{0-0}/A_{0-1}	1.44	1.41	1.66
$\varepsilon_{max}(A_{0-0})/M^{-1}$ cm^{-1}	75 670	73 870	41 000
$\varepsilon_{max}(A_{0-1})/M^{-1}$ cm^{-1}	52 510	52 150	24 700
λ_{em}/nm	626	626	620
$\Delta\tilde{\nu}_{Stokes}$/cm^{-1}	1196	1183	878
FLQY[b]	0.16	0.07	0.97
Lifetime[c]	2.6 ns	2.6 ns	6.5 ns
k_{fl} [10^8 s^{-1}][d]	0.62	0.27	1.49
k_{nr} [10^8 s^{-1}][d]	3.23	3.58	0.05

[a] Photostationary state **APC** after UV irradiation for 1 min. [b] Absolute FLQY method using an integrating sphere at an excitation wavelength of 510 nm. [c] The wavelength of the pulsed laser diode is 505.8 nm, and the emission intensity was monitored at 650 nm. [d] Determined according to $k_{fl} = \Phi_{fl}/\tau_{fl}$ and $k_{nr} = 1/\tau_{fl} - k_{fl}$.

of azobenzene.[39] The photoisomerization efficiency of reference azobenzene **2** is calculated to be about 70% according to the evaluation of both NMR and UV-vis experiments (Fig. S5–7, ESI†).

The basic optical properties of PBI cyclophane **APC** were then examined by UV-vis absorption and fluorescence spectroscopy in $CHCl_3$ due to its good solubility in this solvent. As shown in Fig. 2b, the characteristic absorption peaks of A_{0-0} and A_{0-1} vibronic transitions are located at 589 and 550 nm, respectively. The A_{0-0}/A_{0-1} ratio, which can be used as an indicator for revealing H- or J-aggregates for PBI chromophores,[34,40] amounts to 1.50. This value is smaller than that of **Ref-PBI** (1.66, Table 1) and indicates weak exciton–vibrational coupling between the PBI chromophores within the cyclophane. The fluorescence spectrum was obtained by excitation in the PBI $S_0 \rightarrow S_1$ absorption region (λ_{ex} = 550 nm), which showed an emission band in the wavelength region of 560–800 nm (Fig. 2b, magenta line).

The photoisomerization experiments of **APC** were then studied by UV-vis absorption, fluorescence and NMR spectroscopy. As shown in Fig. S8a,† after 10 s UV irradiation (λ_{ex} = 350 nm), the absorption peak at 328 nm ascribed to the *trans*-Azo moiety drops but remains almost unchanged in the following longer irradiation time (30 s and 60 s), which proves that a photostationary state is achieved under these irradiation conditions. The corresponding *cis*-Azo absorption peak, which should be observed at about 440 nm (Fig. 2a), is buried under the $S_0 \rightarrow S_2$ absorption band of the PBI units (λ_{max} = 455 nm). The PBI emission shows only a slight decrease after UV irradiation (Fig. S9, ESI†). The *trans* → *cis* transformation ratio of **APC** in chloroform was calculated to be about 22% based on NMR and UV-vis spectra (Fig. S10 and S11, ESI†). Although the photoisomerization shows good reversibility (Fig. S8c and d, ESI†), the relatively low conversion rate limits its potential application.[41]

However, the *trans* → *cis* conversion ratio could be significantly enhanced by changing the solvent. Accordingly, time-dependent UV-vis spectra of cyclophane **APC** after variable UV irradiation time were recorded in dichloromethane. As shown in Fig. 3a, the absorption peak at 343 nm assigned to *trans*-Azo decreases significantly upon UV irradiation. After 70 s UV irradiation, the photostationary state is achieved, showing negligible absorption change compared with that after 60 s irradiation. However, due to the poor solubility of **APC** in dichloromethane at the NMR concentration scale (mM), the *trans* → *cis* transformation efficiency of **APC** could be only estimated by UV-vis spectroscopy (Fig. S12, ESI†), giving a value of 80%. Notably, the absorption maximum of PBI shows a small bathochromic shift from 583 to 586 nm, and the A_{0-0}/A_{0-1} ratio is slightly reduced from 1.44 to 1.41 (Table 1) upon photoisomerization, which reveals an increase of the exciton coupling strength between the two PBI chromophores within the cyclophane due to the decrease of the PBI–PBI distance. In addition, the quantum yield of **APC** decreased from 16% to 7% after UV irradiation (Table 1) accompanied by a decrease of fluorescence emission intensity. As shown in Fig. 3c, fluorescence intensity decreases drastically in the first 10 s of irradiation and reaches the final photostationary state after 60 s, which shows a weakened fluorescence intensity compared with the initial state.

Back-switching from PSS-**APC** to *trans*-**APC** was studied by time-dependent absorption and emission spectroscopy to evaluate the reversible capability. After irradiating with visible light for 30 min (Fig. 3b), PSS-**APC** can be almost totally switched back to the initial thermodynamically stable *trans*-

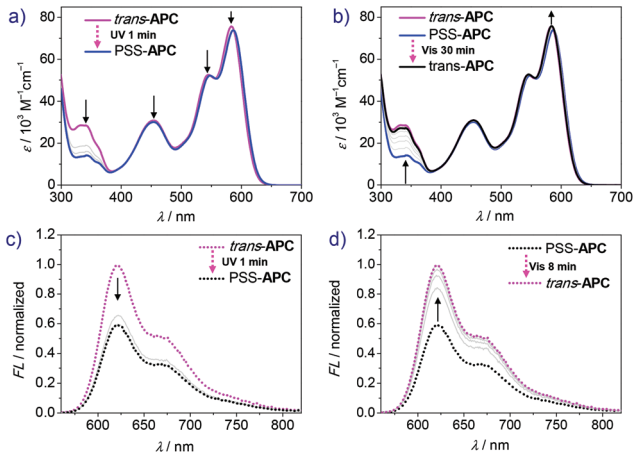

Fig. 3 Time-dependent photoisomerization experiments based on UV-vis and fluorescence spectroscopy, [**APC**] = 8.6 × 10^{-6} M in DCM, 298 K. (a) The changes of UV-vis spectra after different UV irradiation time. The spectra of the initial *trans*-**APC** state (solid magenta line) and the final PSS state after 70 s irradiation (solid blue line) are shown. (b) The change of UV-vis spectra after different visible light irradiation time. The initial PSS-**APC** (solid blue line), the final state after 30 min visible light irradiation (solid black line) and the thermodynamically stable *trans*-**APC** (solid magenta line) are shown. (c) The change of fluorescence spectra after different UV irradiation time showing the initial *trans*-**APC** (dashed magenta line) and the final PSS-**APC** after 60 s UV irradiation (dashed black line). (d) The change of fluorescence spectra after different visible light irradiation time showing the UV-illuminated photostationary state (dashed black line) and the final state after 8 min visible light irradiation (dashed magenta line). All the grey lines represent intermediate states under different irradiation time.

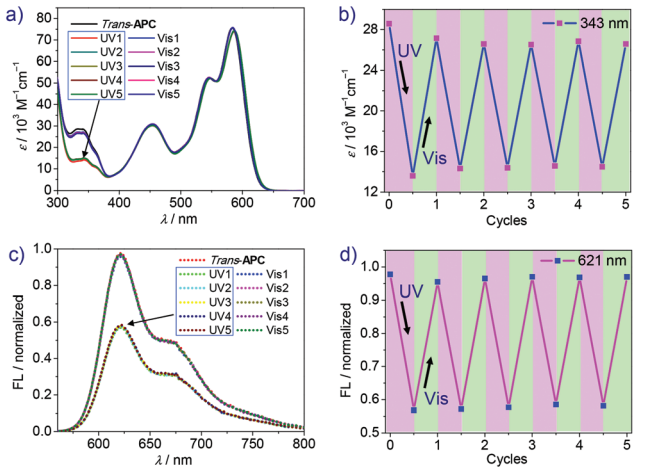

Fig. 4 Absorption and emission spectrum switching under alternate UV (350 nm) and visible light irradiation. (a) UV-vis absorption spectra of cyclophane **APC** ([**APC**] = 8.6 × 10^{-6} M in DCM). (b) Change of azobenzene absorption at 343 nm. (c) Fluorescence spectra of **APC**. (d) The emission intensity changes at 621 nm. The UV irradiation time is 60 s for each cycle and the visible light irradiation time is 10 min.

state. In our experiments, fluorescence intensity shows a faster recovery rate (only 8 minutes) than the recovery of the initial UV-vis absorption spectrum because of the lower concentration of cyclophane **APC** for fluorescence measurements, which is an order of magnitude smaller than the one applied in UV-vis spectroscopy. By alternate UV and visible light irradiation (Fig. 4), *trans*- and PSS-**APC** states were successfully switched for five cycles, revealing no indication of efficiency decrease or degradation as demonstrated by the absorption intensity at 343 nm ascribed to *trans*-azobenzene (Fig. 4b) as well as by the PBI emission band at 621 nm (Fig. 4d), which indicates a fatigue resistance photoswitch.

The optical properties of **APC** before and after UV irradiation are summarized in Table 1. The excitation spectrum (Fig. 2b, blue line) reveals that the azobenzene absorption also contributes to the PBI emission. In addition, the fluorescence quantum yield of **APC** by excitation of both the azobenzene part (λ_{Ex} = 350 nm) and the PBI part (λ_{Ex} = 510 nm) gave the same value of 16% (Table S1, ESI†), which reveals an energy transfer process from the excited *trans*-Azo* to PBI. This conclusion is in agreement with the work of Müllen and coworkers.[42] They have proved an efficient energy transfer in an Azo–PBI dendrimer from the excited Azo* moiety to the PBI chromophore by fluorescence and ultrafast transient absorption spectroscopy. It was also shown that after energy transfer, the excited PBI undergoes a radiative relaxation to the ground state with the lifetime (several nanoseconds) as observed when only the PBI unit is excited at 570 nm. For our system, both the fluorescence quantum yield and lifetime of **APC** are obviously smaller than those of **Ref-PBI** (Table 1), which indicates an efficient nonradiative decay process.

To gain insight into the molecular geometries and electronic structures of *trans–trans* **APC** and *cis–cis* **APC**, theoretical calculations were carried out using density functional theory (DFT) at the B3LYP 6-31 G(d,p) level.[43] The geometry-optimized structures are shown in Fig. 5. Accordingly, for the *trans–trans* isomer, the distance between the planes of the two PBI chromophores is about 12 Å (Fig. 5a), which explains the weak exciton coupling as is evident from the A_{0-0}/A_{0-1} ratio in the absorption spectrum of *trans*-**APC**, which is slightly smaller than that of individual **Ref-PBI** (Table 1). For the *cis–cis* state, the distance between the two PBI planes is shortened to 7.6 Å (Fig. 5c), which is reflected in the further decrease of the A_{0-0}/A_{0-1} ratio from 1.44 to 1.41 (Table 1). A comparison of the quantum yields of *trans*-**APC** and PSS-**APC** with the values obtained for PBI cyclophanes with a similar interchromophoric distance but without the presence of an azobenzene moiety[28] reveals a strong decrease of the quantum yield for *trans*-**APC** and PSS-**APC**. Hence, the azobenzene moiety used by us leads to pronounced fluorescence quenching. We attribute this to an electron transfer from the azobenzene moiety to the photoexcited PBI moiety. An MO analysis (Fig. S14 and S15, ESI†) reveals pairwise orbitals due to slight differences in the respective PBI and Azo units. Both frontier orbitals, *i.e.*, the HOMO (and HOMO−1) as well as LUMO (and LUMO+1) are located on the PBI subunits. However, the orbitals HOMO−2 and HOMO−3 of *cis*-**APC**, both of which have a large coefficient on the azobenzene moiety (Fig. 5e and Fig. S15, ESI†), are only ~0.1 eV lower in energy than the HOMO

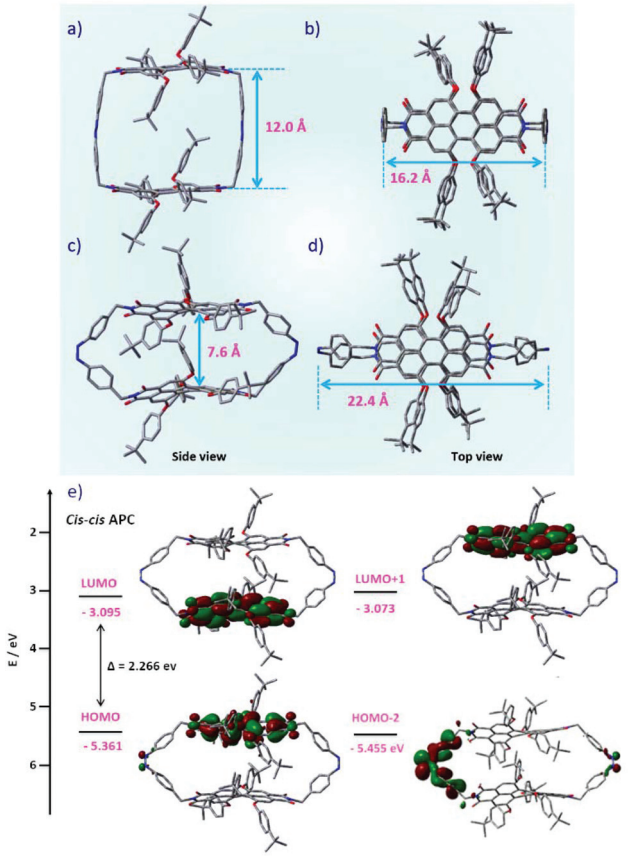

Fig. 5 Density functional theory calculated structures of (a and b) *trans–trans* **APC** and (c and d) *cis–cis* **APC**. (e) Illustration of energy levels and molecular orbitals of *cis–cis* **APC**. Gaussian 09, B3LYP/6-31G (d,p) level. All hydrogen atoms are omitted for clarity.

(Fig. S13†), which is located at one of the PBI chromophores (Fig. 5e). Thus, considering conformational motions that are pronounced for both the *cis*-Azo and the tetraphenoxy-PBI[44] subunits, an electron can be transferred from the azobenzene moiety to the PBI moiety after photoexcitation of PBI. However, the energy difference for *trans*-**APC** (~0.5 eV, Fig. S13†) is larger than that for *cis*-**APC**. Therefore, while photo-induced electron transfer is the most likely origin of the strong fluorescence quenching of *cis*-**APC**, another quenching mechanism might be operative for *trans*-**APC**.

Because some PBI cyclophanes studied in our earlier work were excellent hosts for several polycyclic aromatic hydrocarbons[26,45] and even for some alkaloids,[29] we also performed UV-vis and fluorescence titration experiments with a variety of guests (Fig. S16 and S17†), *e.g.*, naphthalene, 1,5-dimethoxynaphthalene, 1,1′-biphenyl, 1-phenylnaphthalene, anthracene, phenanthrene, and pyrene, for both *trans*-**APC** and PSS-**APC** states in dichloromethane. However, no evidence for binding was observed, which suggests that neither the cavities formed by *trans*- nor those by *cis*-azobenzene pillar units provide a suitable preorganization for the complexation of aromatic guest molecules.

Conclusions

In summary, an azobenzene-bridged perylene bisimide cyclophane was synthesized and characterized. Our spectroscopic studies in combination with theoretical calculations indicate a pronounced electronic communication between the azobenzene and PBI chromophores, as is evident from the significant fluorescence quenching of the PBI units. Notably, a photoisomerization of azobenzene is observed upon irradiation with UV light. The reversible photoswitching of the azobenzene chromophore under UV and visible light irradiation is accompanied by pronounced structural and electronic changes of **APC**, which significantly altered the cavity size of the macrocycle and the emission behaviour of the perylene bisimide chromophores. Accordingly, this work provides insights into the design of photoresponsive luminescent macrocycles and supramolecular elements based on PBI and azobenzene.

Conflicts of interest

There are no conflicts to declare.

Acknowledgements

We are thankful for the fund from the Chinese Academy of Sciences for supporting a visiting research of G. O. at Universität Würzburg.

Notes and references

1 J. M. Lehn, Supramolecular Chemistry—Scope and Perspectives Molecules, Supermolecules, and Molecular Devices (Nobel Lecture), *Angew. Chem., Int. Ed. Engl.*, 1988, **27**, 89–112.
2 Q. He, G. I. Vargas-Zúñiga, S. Kim, S. Kim and J. L. Sessler, Macrocycles as Ion Pair Receptors, *Chem. Rev.*, 2019, **119**, 9753–9835.
3 J. A. Faiz, V. Heitz and J. P. Sauvage, Design and Synthesis of Porphyrin-containing Catenanes and Rotaxanes, *Chem. Soc. Rev.*, 2009, **38**, 422–442.
4 H. W. Schmidt and F. Würthner, A Periodic System of Supramolecular Elements, *Angew. Chem., Int. Ed.*, 2020, **59**, 8766–8775.
5 X. Yan, F. Wang, B. Zheng and F. Huang, Stimuli-responsive Supramolecular Polymeric Materials, *Chem. Soc. Rev.*, 2012, **41**, 6042–6065.
6 C. D. Jones and J. W. Steed, Gels with Sense: Supramolecular Materials that Respond to Heat, Light and Sound, *Chem. Soc. Rev.*, 2016, **45**, 6546–6596.
7 J. Boekhoven and S. I. Stupp, 25th Anniversary Article: Supramolecular Materials for Regenerative Medicine, *Adv. Mater.*, 2014, **26**, 1642–1659.

8 Y. Wang, H. Xu and X. Zhang, Tuning the Amphiphilicity of Building Blocks: Controlled Self–Assembly and Disassembly for Functional Supramolecular Materials, *Adv. Mater.*, 2009, **21**, 2849–2864.
9 D. B. Amabilino, D. K. Smith and J. W. Steed, Supramolecular Materials, *Chem. Soc. Rev.*, 2017, **46**, 2404–2420.
10 B. Shirinfar, N. Ahmed, Y. S. Park, G. S. Cho, I. S. Youn, J. K. Han, H. G. Nam and K. S. Kim, Selective Fluorescent Detection of RNA in Living Cells by Using Imidazolium-Based Cyclophane, *J. Am. Chem. Soc.*, 2013, **135**, 90–93.
11 J. H. Tang, Y. Sun, Z. L. Gong, Z. Y. Li, Z. X. Zhou, H. Wang, X. P. Li, M. L. Saha, Y. W. Zhong and P. J. Stang, Temperature-Responsive Fluorescent Organoplatinum(II) Metallacycles, *J. Am. Chem. Soc.*, 2018, **140**, 7723–7729.
12 K. Mase, Y. Sasaki, Y. Sagara, N. Tamaoki, C. Weder, N. Yanai and N. Kimizuka, Stimuli–Responsive Dual–Color Photon Upconversion: A Singlet–to–Triplet Absorption Sensitizer in a Soft Luminescent Cyclophane, *Angew. Chem., Int. Ed.*, 2018, **57**, 2806–2810.
13 M. Dumartin, M. C. Lipke and J. F. Stoddart, A Redox-Switchable Molecular Zipper, *J. Am. Chem. Soc.*, 2019, **141**, 18308–18317.
14 S. Erbas-Cakmak, D. A. Leigh, C. T. McTernan and A. L. Nussbaumer, Artificial Molecular Machines, *Chem. Rev.*, 2015, **115**, 10081–10206.
15 K. Kurihara, K. Yazaki, M. Akita and M. Yoshizawa, A Switchable Open/closed Polyaromatic Macrocycle that Shows Reversible Binding of Long Hydrophilic Molecules, *Angew. Chem., Int. Ed.*, 2017, **56**, 11360–11364.
16 H. Wu, Y. Chen, L. Zhang, O. Anamimoghadam, D. K. Shen, Z. C. Liu, K. Cai, C. Pezzato, C. L. Stern, Y. Liu and J. F. Stoddart, A Dynamic Tetracationic Macrocycle Exhibiting Photoswitchable Molecular Encapsulation, *J. Am. Chem. Soc.*, 2019, **141**, 1280–1289.
17 S. T. J. Ryan, J. del Barrio, R. Suardiaz, D. F. Ryan, E. Rosta and O. A. Scherman, A Dynamic and Responsive Host in Action: Light-Controlled Molecular Encapsulation, *Angew. Chem., Int. Ed.*, 2016, **55**, 16096–16100.
18 G. Szaloki, V. Croue, V. Carre, F. Aubriet, O. Aleveque, E. Levillain, M. Allain, J. Arago, E. Orti, S. Goeb and M. Salle, Controlling the Host-Guest Interaction Mode through a Redox Stimulus, *Angew. Chem., Int. Ed.*, 2017, **56**, 16272–16276.
19 F. Würthner, C. R. Saha-Möller, B. Fimmel, S. Ogi, P. Leowanawat and D. Schmidt, Perylene Bisimide Dye Assemblies as Archetype Functional Supramolecular Materials, *Chem. Rev.*, 2016, **116**, 962–1052.
20 C. Li and H. Wonneberger, Perylene Imides for Organic Photovoltaics: Yesterday, Today, and Tomorrow, *Adv. Mater.*, 2012, **24**, 613–636.
21 H. Langhals and R. Ismael, Cyclophanes as Model Compounds for Permanent, Dynamic Aggregates – Induced Chirality with Strong CD Effects, *Eur. J. Org. Chem.*, 1998, 1915–1917.
22 J. Feng, Y. Zhang, C. Zhao, R. Li, W. Xu, X. Li and J. Jiang, Cyclophanes of Perylene Tetracarboxylic Diimide with Different Substituents at Bay Positions, *Chem. – Eur. J.*, 2008, **14**, 7000–7010.
23 K. E. Brown, W. A. Salamant, L. E. Shoer, R. M. Young and M. R. Wasielewski, Direct Observation of Ultrafast Excimer Formation in Covalent Perylenediimide Dimers Using Near-Infrared Transient Absorption Spectroscopy, *J. Phys. Chem. Lett.*, 2014, **5**, 2588–2593.
24 W. Kim, A. Nowak-Król, Y. Hong, F. Schlosser, F. Würthner and D. Kim, Solvent-Modulated Charge-Transfer Resonance Enhancement in the Excimer State of a Bay-Substituted Perylene Bisimide Cyclophane, *J. Phys. Chem. Lett.*, 2019, **10**, 1919–1927.
25 F. Schlosser, M. Moos, C. Lambert and F. Würthner, Redox–switchable Intramolecular π–π–Stacking of Perylene Bisimide Dyes in a Cyclophane, *Adv. Mater.*, 2013, **25**, 410–414.
26 P. Spenst and F. Würthner, A Perylene Bisimide Cyclophane as a "Turn–On" and "Turn–Off" Fluorescence Probe, *Angew. Chem., Int. Ed.*, 2015, **54**, 10165–10168.
27 D. Bialas, C. Brüning, F. Schlosser, B. Fimmel, J. Thein, V. Engel and F. Würthner, Exciton–Vibrational Couplings in Homo– and Heterodimer Stacks of Perylene Bisimide Dyes within Cyclophanes: Studies on Absorption Properties and Theoretical Analysis, *Chem. – Eur. J.*, 2016, **22**, 15011–15018.
28 J. Rühe, D. Bialas, P. Spenst, A.-M. Krause and F. Würthner, Perylene Bisimide Cyclophanes: Structure–Property Relationships upon Variation of the Cavity Size, *Org. Mater.*, 2020, **02**, 149–158.
29 M. Sapotta, A. Hofmann, D. Bialas and F. Würthner, A Water-Soluble Perylene Bisimide Cyclophane as a Molecular Probe for the Recognition of Aromatic Alkaloids, *Angew. Chem., Int. Ed.*, 2019, **58**, 3516–3520.
30 M. Sapotta, P. Spenst, C. R. Saha-Möller and F. Würthner, Guest-mediated Chirality Transfer in the Host–guest Complexes of an Atropisomeric Perylene Bisimide Cyclophane Host, *Org. Chem. Front.*, 2019, **6**, 892–899.
31 P. Spenst, R. M. Young, M. R. Wasielewski and F. Würthner, Guest and Solvent Modulated Photo-driven Charge Separation and Triplet Generation in A Perylene Bisimide Cyclophane, *Chem. Sci.*, 2016, **7**, 5428–5434.
32 T. A. Barendt, W. K. Myers, S. P. Cornes, M. A. Lebedeva, K. Porfyrakis, I. Marques, V. Felix and P. D. Beer, The Green Box: An Electronically Versatile Perylene Diimide Macrocyclic Host for Fullerenes, *J. Am. Chem. Soc.*, 2020, **142**, 349–364.
33 J. Seibt, T. Winkler, K. Renziehausen, V. Dehm, F. Würthner, H. D. Meyer and V. Engel, Vibronic Transitions and Quantum Dynamics in Molecular Oligomers: A Theoretical Analysis with an Application to Aggregates of Perylene Bisimides, *J. Phys. Chem. A*, 2009, **113**, 13475–13482.
34 F. C. Spano, The Spectral Signatures of Frenkel Polarons in H- and J-Aggregates, *Acc. Chem. Res.*, 2010, **43**, 429–439.

35 C. Zhang and N. Jiao, Copper-catalyzed Aerobic Oxidative Dehydrogenative Coupling of Anilines Leading to Aromatic Azo Compounds Using Dioxygen as An Oxidant, *Angew. Chem., Int. Ed.*, 2010, **49**, 6174–6177.
36 D. Dotcheva, M. Klapper and K. Müllen, Soluble Polyimides Containing Perylene Units, *Macromol. Chem. Phys.*, 1994, **195**, 1905–1911.
37 A. Nowak-Król and F. Würthner, Progress in the Synthesis of Perylene Bisimide Dyes, *Org. Chem. Front.*, 2019, **6**, 1272–1318.
38 P. Osswald, M. Reichert, G. Bringmann and F. Würthner, Perylene Bisimide Atropisomers: Synthesis, Resolution, and Stereochemical Assignment, *J. Org. Chem.*, 2007, **72**, 3403–3411.
39 H. M. D. Bandara and S. C. Burdette, Photoisomerization in Different Classes of Azobenzene, *Chem. Soc. Rev.*, 2012, **41**, 1809–1825.
40 F. Würthner, T. E. Kaiser and C. R. Saha-Möller, J-aggregates: from Serendipitous Discovery to Supramolecular Engineering of Functional Dye Materials, *Angew. Chem., Int. Ed.*, 2011, **50**, 3376–3410.
41 A. A. Beharry and G. A. Woolley, Azobenzene Photoswitches for Biomolecules, *Chem. Soc. Rev.*, 2011, **40**, 4422–4437.
42 T. T. Nguyen, D. Turp, D. Wang, B. Nolscher, F. Laquai and K. Müllen, A Fluorescent, Shape-Persistent Dendritic Host with Photoswitchable Guest Encapsulation and Intramolecular Energy Transfer, *J. Am. Chem. Soc.*, 2011, **133**, 11194–11204.
43 M. J. Frisch, *et al.*, *Gaussian 16 Rev. C. 01*.
44 E. Fron, G. Schweitzer, P. Osswald, F. Würthner, P. Marsal, D. Beljonne, K. Müllen, F. C. De Schryver and M. Van der Auweraer, Photophysical Study of Bay Substituted Perylenediimides, *Photochem. Photobiol. Sci.*, 2008, **7**, 1509–1521.
45 P. Spenst, A. Sieblist and F. Würthner, Perylene Bisimide Cyclophanes with High Binding Affinity for Large Planar Polycyclic Aromatic Hydrocarbons: Host-Guest Complexation versus Self-Encapsulation of Side Arms, *Chem. – Eur. J.*, 2017, **23**, 1667–1675.